Use of picosecond Kerr-gated Raman spectroscopy to suppress signals from both surface and deep layers in bladder and prostate tissue

Maria Consuelo Hart Prieto
Gloucestershire Royal Hospital
Biophotonics Research Group
Pullman Court
Great Western Road
Gloucester GL 1 3NN
United Kingdom

Pavel Matousek
Michael Towrie
Anthony William Parker
CCLRC Rutherford Appleton Laboratory
Central Laser Facility
Didcot, Oxfordshire OX11 0QX
United Kingdom

Mark Wright
Bristol Royal Infirmary
Bristol BS2 8HW
United Kingdom

Alistair William Ritchie
Gloucestershire Royal Hospital
Great Western Road
Gloucester GL1 3NN
United Kingdom

Nicholas Stone
Gloucestershire Royal Hospital
Biophotonics Research Group
Pullman Court
Great Western Road
Gloucester GL1 3NN
United Kingdom
E-mail: n.stone@medical-research-centre.com

Abstract. Raman spectroscopy is an optical technique able to interrogate biological tissues, giving us an understanding of the changes in molecular structure that are associated with disease development. The Kerr-gated Raman spectroscopy technique uses a picosecond pulsed laser as well as fast temporal gating of collected Raman scattered light. Prostate samples for this study were obtained by taking a chip at the transurethral resection of the prostate (TURP), and bladder samples from a biopsy taken at transurethral resection of bladder tumor (TURBT) and TURP. Spectra obtained through the bladder and prostate gland tissue, at different time delays after the laser pulse, clearly show change in the spectra as depth profiling occurs, eventually showing signals from the uric acid cell and urea cell, respectively. We show for the first time, using this novel technique, that we are able to obtain spectra from different depths through both the prostate gland and the bladder. This has major implications in the future of Raman spectroscopy as a tool for diagnosis. With the help of Raman spectroscopy and Kerr gating, it may be possible to pick up the spectral differences from a small focus of adenocarcinoma of the prostate gland in an otherwise benign gland, and also stage the bladder cancers by assessing the base of the tumor post resection. © 2005 Society of Photo-Optical Instrumentation Engineers. [DOI: 10.1117/1.1991848]

1 Introduction

1.1 Bladder

Each year there are 9000 cases of bladder cancer diagnosed in men and 3600 diagnosed in women in the United Kingdom. It is the fourth most common cancer in men and the eighth most common in women (the incidence is 8% in men and 3% in women[1]). There has, however, been a reduction in the age standardized incidence since the 1980s. This is thought to be due to the reduction in smoking and the banning of aromatic amines in the 1980s, both of which are known risk factors for the development of bladder cancer.

The vast majority of bladder cancers are transitional cell carcinomas of the bladder, and the majority of these are superficial. Bladder cancer is usually diagnosed by means of a cystoscopy and biopsy under general anaesthetic. Once diagnosed, patients are then staged using the tumor-nodes-metastases (TNM) classification and entered into a surveillance program, if no further treatment is required. The surveillance program involves six monthly to yearly cystoscopies for at least ten years.

Unfortunately, some of the bladder tumors, especially carcinoma *in situ* and flat superficial tumors, can look just like cystitis, or normal bladder.

1.2 Prostate Gland

The majority of men will suffer with symptoms related to diseases of the prostate gland at some point in their lives, with prostate cancer being the one of main concern. Adenocarcinoma of the prostate gland (CaP) is the most frequently diagnosed noncutaneous cancer affecting Western men.[2] Most (95%) of the cancers affecting the prostate gland are adeno-

Address all correspondence to Nicholas Stone, Gloucestershire Hospitals NHS Trust, Cranfield Postgrad Medical School-Great Western Rd., Gloucester, Gloucestershire GL1 3NN, Great Britain. Tel: 44 1452 395712; Fax: 44 1452 395713; E-mail: n.stone@medical-research-centre.com

carcinomas, the other 5% are made up of the following: transitional cell carcinoma, neuroendocrine carcinoma, sarcoma, and lymphoma. 40% of men aged between 60 and 70 years have microscopic foci of well-differentiated CaP. It is the second leading cause of cancer-related death in men in Western Europe and North America,[2] with 3 to 5% of men dying of CaP. It is also a major cause of morbidity and healthcare-related costs with 10% of men diagnosed with CaP developing clinical disease.[2]

CaP is diagnosed by means of an abnormal digital rectal examination (DRE) and/or a raised level of serum prostate-specific antigen (PSA). Either of these will lead onto transrectal ultrasonography (TRUS) and biopsy. The biopsies are taken randomly, with targeting if a lesion is suspected on TRUS. Unfortunately, the biopsies have a high number of false negatives, and therefore a cancer can remain undiagnosed. These false negatives are mainly due to sampling error (CaP is present as a small focus within the prostate gland and the biopsy has missed it). It has been shown that even if a man has two sets of negative biopsies with a persistently raised PSA, he has a 10% risk of having a cancer found on the third biopsy.

PSA measurement also comes with its own problems, in that although it is highly sensitive, it is not very specific. PSA can also be raised in the following: benign prostate hyperplasia (BPH), prostatitis, acute urinary retention (AUR), and urinary tract infection (UTI), as well as following recent urethral instrumentation, catheterization, prostatic biopsy, and DRE.

The ideal would be to diagnose CaP at an early stage when the PSA is within the range of 2.5 to 10 ng/ml; this would increase the chances of cure with radical treatment. The reality, given the low specificity of both the PSA, and the TRUS and biopsy, is that many of the cancers are diagnosed when a cure is not possible.

1.3 Raman Spectroscopy

Raman spectroscopy is an optical technique that can act to interrogate biological tissues with chemical specificity. In doing so, it gives us an understanding of the changes in the molecular structure that is associated with disease. With this in mind, it was felt that Raman spectroscopy could be used to distinguish between pathologies within the bladder and the prostate gland. By the start of the 1990s, various groups were using Raman spectroscopy to distinguish between normal and neoplastic tissue. The first studies looked at differentiating between normal tissue and advanced cancers in the breast[3] and gynecological organs.[4,5] As techniques were refined, interest moved to diagnosing neoplastic change at progressively earlier stages. To date, *in vitro* studies have also been undertaken to differentiate between different pathologies in a number of other tissues including colon,[6,7] esophagus,[8–10] brain,[11] skin,[12,13] lung,[14] and larynx.[15]

It has already been shown that Raman spectroscopy can be used to distinguish between different pathologies within the bladder and the prostate gland. This, however, has been exclusively *in vitro*.[16,17]

In view of previous studies, Raman spectroscopy is thought to have the potential for minimally invasive detection of malignancies and premalignancies within the bladder and the prostate gland. A problem with this is the inability to obtain spectra from significantly beneath the surface (more than of the order of 100 μm).[18] This is needed to ascertain whether there has been any local invasion of the disease in the case of the bladder, or to find a focus of adenocarcinoma in an otherwise benign prostate gland.

1.4 Kerr Gating

A Raman signal from depths within tissues tends to be diminished by elastic scattering, and therefore the surface signal is usually significantly stronger. A possible way to overcome this is by temporal gating techniques such as picosecond Kerr gating. The Kerr-gating technique uses excitation with a picosecond pulsed laser, in combination with a fast temporal gating of the Raman scattered light. The scattered light is collected at various time delays following the laser pulse.

The ability of depth probing using Raman is determined by two stages: 1. the laser photons have to be able to migrate to a given depth within the tissue; and 2. the Raman photons that have been produced have to migrate back to the surface.

In this way Raman spectra from differing depths within the tissue will emerge at different times, thereby making their separation feasible.[19]

There have been studies utilizing the Kerr-gating technique to improve on Raman spectra obtained from bone interiors,[20] as well as test experiments demonstrating the depth resolving power of the Raman Kerr-gating concept on artificially prepared samples.[19] This study is designed to expand on this work by studying the facility of Kerr-gated Raman spectroscopy to measure biochemical data from depths of a few millimeters in soft tissue. To make certain that a signal has been detected from beneath the tissue layer, specimens with strong and distinct Raman signals have been used. These were also selected for their relevance in urology.

2 Materials and Methods

2.1 Subjects

We obtained approval from the Gloucestershire Research Ethics Committee to obtain samples for experimentation using Raman spectroscopy. The samples used for this study were taken following fully informed consent.

2.2 Tissue Collection and Preparation

Prostate samples were obtained by taking an extra core at prostate biopsy procedures, or a chip at trans-urethral resection of the prostate (TURP). The prostate sample used in this study was assessed histopathologically to be benign prostatic hyperplasia. Bladder samples were collected at cystoscopic procedures including TURP (normal biopsies) and during trans-urethral resection of bladder tumor (TURBT). The bladder sample used was histologically normal and included the urothelial and subsurface layers. The samples were then snap-frozen in liquid nitrogen and transferred to an $-80\,°C$ freezer for storage.

At the time of the experiment, the tissue was passively warmed to room temperature and placed either on a cell containing urea, or on one containing uric acid. Urea and uric acid were chosen because they can be found within the bladder and prostate gland, and may also form crystals. Urea and
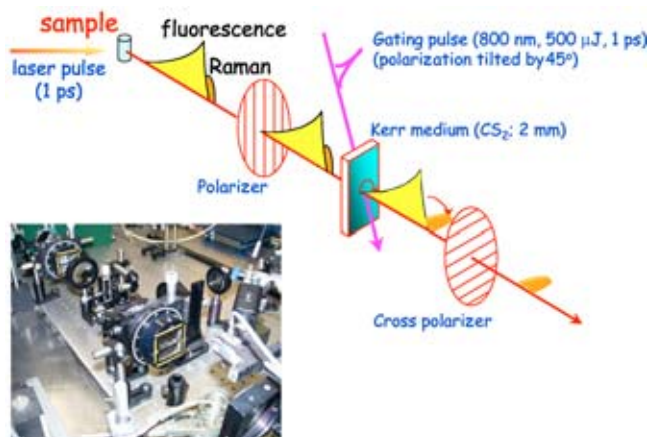
Fig. 1 A schematic diagram and photograph showing the Kerr-gated Raman system at the Rutherford Appleton Laboratory (RAL).

uric acid are also very strongly Raman active, and were chosen to allow a demonstration of probing of Raman spectra at depths through the tissue samples.

2.3 Instrumentation

The Kerr-gating system is based on the high throughput 4-ps optical Kerr shutter that has been described in previous publications by Matousek et al.[21,22] The Kerr gate is made up of two crossed polarizers (41×41 mm, Glan Taylor polarizers) and a Kerr medium consisting of a 2-mm optical cell that is filled with CS_2 (see Fig. 1).

When the gate is closed, the light from the sample is blocked as the polarizers are in cross orientation. When the gate is open, the light collected from the sample has its polarization rotated to allow it to pass through the cross polarizer. The gate is opened by a short 1-ps gating pulse at 800 nm. This bypasses the polarizers and creates a transient anisotropy within the Kerr medium, this then acts to polarize the light from the sample.

The spectra were collected using a conventional Raman spectrometer (Spex, Triplemate). To prevent residual elastically scattered light from the 488-nm probe laser entering the spectrometer, a Kaiser holographic notch filter was used. To also prevent the residual 800-nm gating beam scatter from entering, a saturated copper sulphate solution in a 1-cm-thick optical cell was placed in front of the spectrometer slit.

The Raman scattered light was collected in 180-deg geometry using a lens with f number of 2. A water heat-exchanger cooled, deep depletion near-infrared (NIR) CCD (Andor Technology, Belfast, UK, DU420BR-DD) was used to record the Raman spectra from the tissue.

The probe wavelength used was 488 nm, and the pulse duration was 1 ps. The pulse energy at the sample was 5 μJ (1 kHz) corresponding to 5 mW of average power. The beam was focused down to a 300-μm-diam spot.

To demonstrate the ability to obtain Raman spectra from deep layers, we performed two experiments: the first involved placing a bladder sample urothelium upward onto a uric acid cell, and the second involved placing the prostate sample onto a urea cell. Both tissue samples were 1 to 2 mm thick. The cells were made from UV-grade quartz 100 μm thick. The spectra were obtained for 20 s and 5 accumulations at varying distances through the tissue, i.e., at various time delays following the laser probe excitation pulse.

A simple approximation as to the distance traveled by the incident photons in the tissue can be made (the refractive index of the tissue was taken to be 1.4). In a time of 1 ps, the photons will have traversed approximately 0.2 mm of the tissue. This will not necessarily be in a straight line, as the tissue is highly scattering. By taking the scattering coefficient μ_s to be 48 mm^{-1} and the absorption coefficient μ_a to be 1.9 mm^{-1} (for epithelial tissue at 577 nm),[23] an optical depth (OD) can be calculated from

$$OD = \frac{1}{\mu_s + \mu_a}.$$

The approximate optical depth in bladder tissue for 488 nm is 0.02 mm.

3 Results

Figure 2 shows the Raman spectra measured from the bladder on top of the cell containing uric acid. As you can see, the peak intensities change as the temporal position of the Kerr gate is varied. This relates to increasing depth with longer time delays, and hence suggests moving through the urothelium and into the basement membrane and then on into the muscle layer. Eventually, the signal from the tissue is lost, with peaks coming up at approximately 1400 and 1650 cm^{-1}, which are consistent with the main uric acid peaks, as shown in Fig. 3. The peaks in Fig. 2 at 662 and 803 cm^{-1} are consistent with the CS2 of the Kerr gate, and peaks at 1079, 1339, and 1533 cm^{-1} are caused by hot pixels from the CCD detector.

Figure 4 shows the spectra obtained going through the prostate gland tissue and on to the urea cell. As can be seen, the first three spectra are clearly tissue spectra with peaks at 1240, 1445, and 1650 cm^{-1} consistent with protein peaks. The fourth spectrum has lost a lot of the signal, and the following spectra yield the urea peaks clearly seen at 1003 and 1170 cm^{-1}.

Figure 5 shows the spectra obtained from the urea cell to highlight the peaks. The peaks in Fig. 4 at 662 and 803 cm^{-1} are consistent with the CS2, and peaks at 1079, 1339, and 1533 cm^{-1} are consistent with hot pixels from the detector and are consistent throughout all of the spectra.

4 Conclusions

We show for the first time that we are able to obtain spectra from different depths through prostate and bladder tissues by utilizing Kerr-gated Raman spectroscopy. Modeling of the time-dependent photon pathway would provide an enhanced understanding of the depth profiling process. This could have major implications in the future of Raman spectroscopy as a tool for diagnosis. Up until now, we have been able to distinguish between different pathologies within the bladder and the prostate gland by sampling the tissue *in vitro*. This has involved looking at only the surface of the sample.

The prostate gland is usually biopsied via the rectum. This is a painful procedure and can give false negatives. With the help of Raman spectroscopy and Kerr gating, we would po-
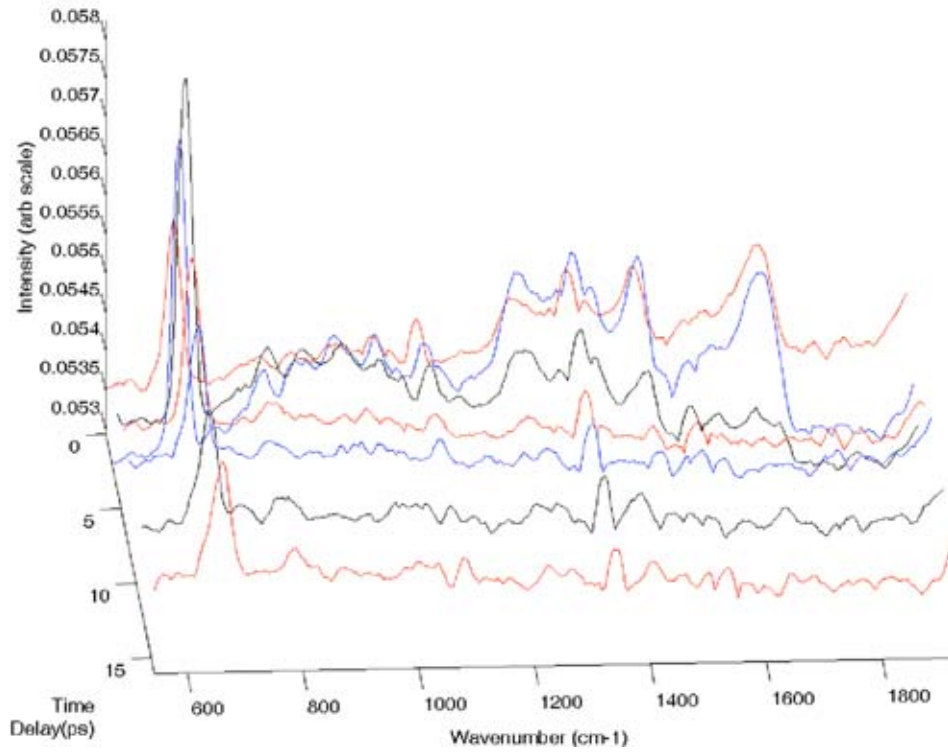
Fig. 2 Raman spectra taken from different depths (by adjusting the delay in opening the Kerr gate) through a sample of bladder on a quartz cell containing uric acid. See text for explanation of peak contributions from the experimental system.
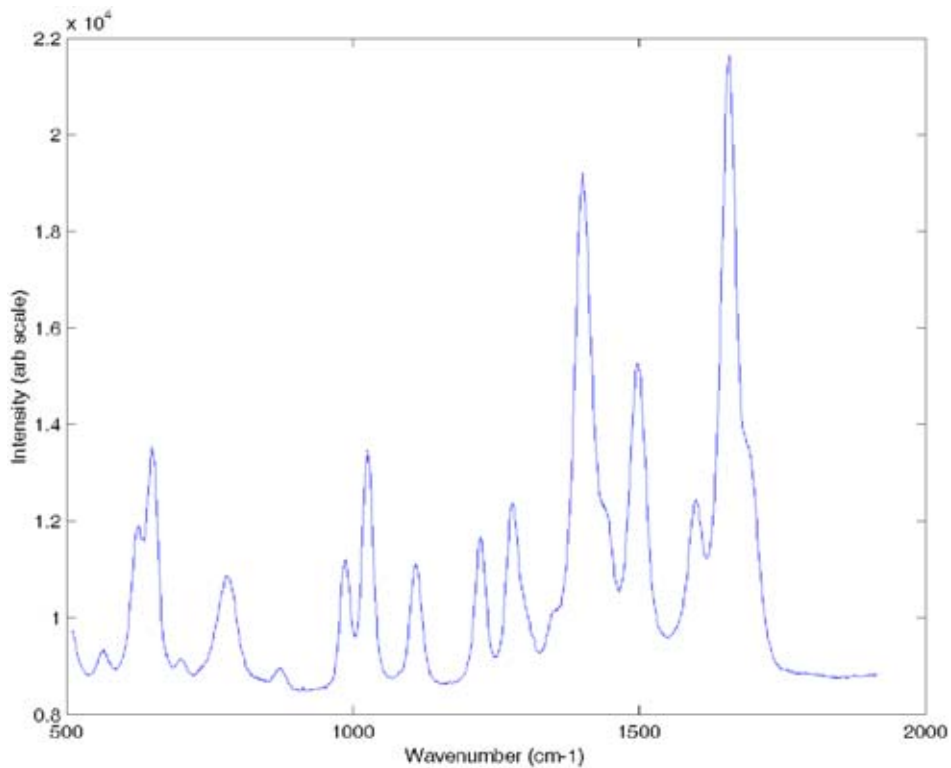

Fig. 3 A Raman spectrum, at a wavelength of 488 nm, taken from a quartz cell containing uric acid.
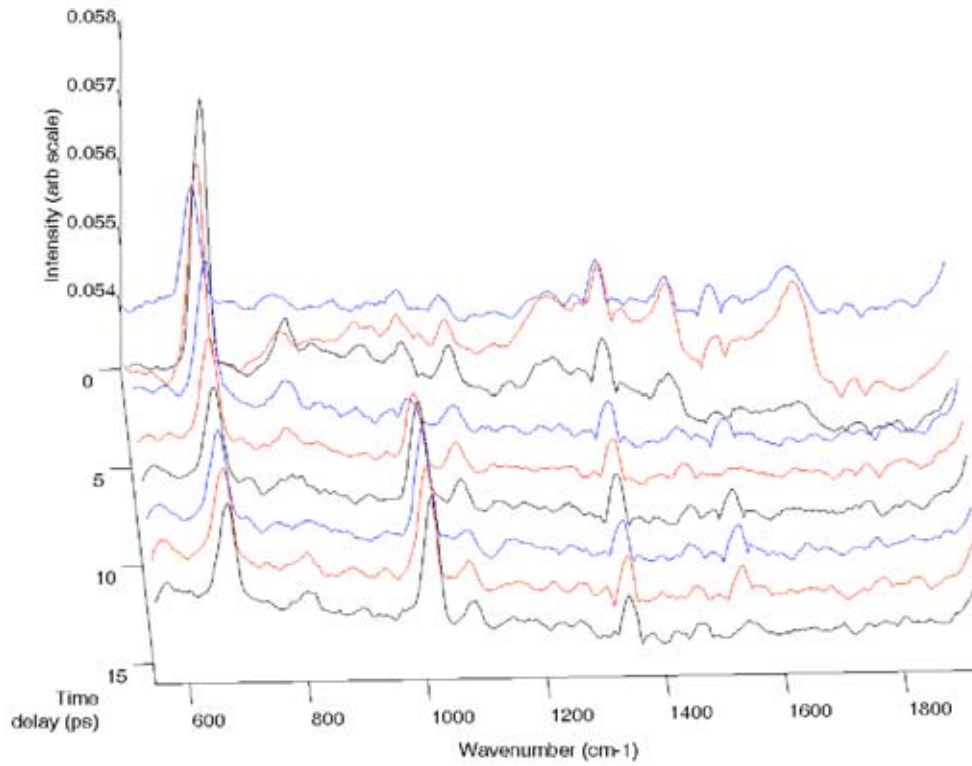
Fig. 4 Raman spectra taken from different depths (by adjusting the delay in opening the Kerr gate) through a sample of prostate gland on a quartz cell containing urea. See text for explanation of peak contributions from the experimental system.
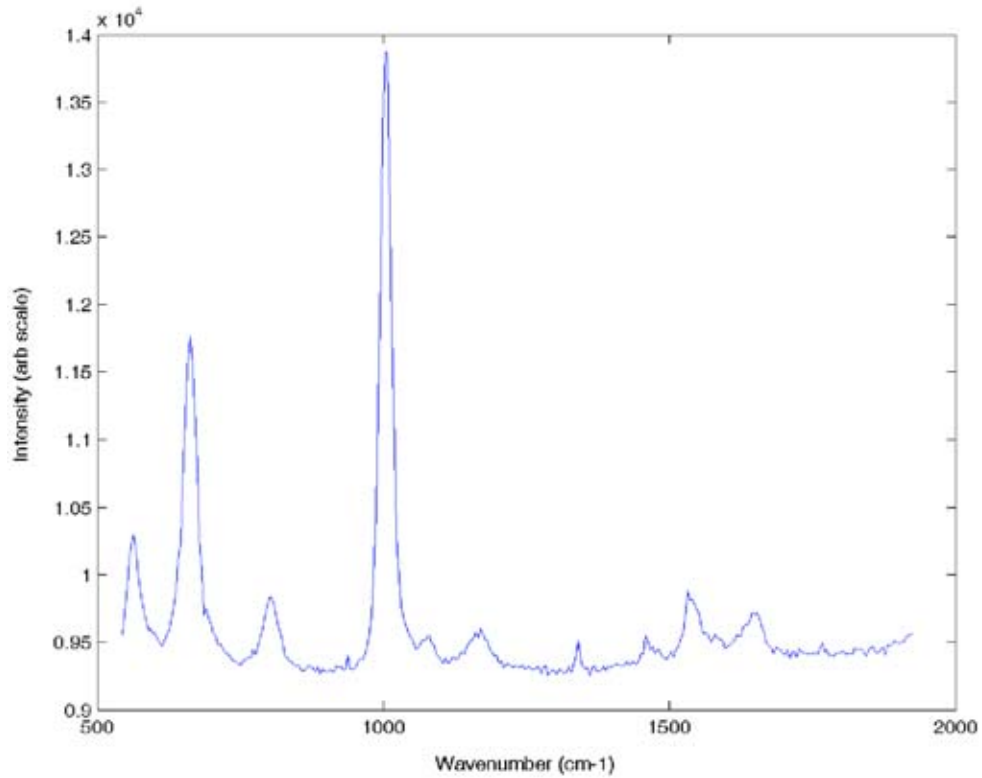

Fig. 5 Raman spectra, at a wavelength of 488 nm, taken from a quartz cell containing urea.

tentially be able to pick up the spectral differences from a small focus of adenocarcinoma of the prostate gland in an otherwise benign gland.

The bladder would also potentially benefit from Raman spectroscopy combined with Kerr gating. We would not only be able to diagnose the presence of a transitional cell carcinoma, but would also be able to assess the stage of the tumor in terms of its extension through the basement membrane and beyond (i.e., greater than a few hundred microns below the surface).

We demonstrate the first principals for the use of Kerr-gated Raman spectroscopy in the diagnosis of biological pathologies. Presently, however, the instrumentation at the Rutherford Appleton Laboratory (RAL) fills two rooms. Therefore, the use of this technique will require technical evolution and advancement before it will be ready for use *in vivo*.

Further studies are planned to demonstrate the facility of the technique to discriminate between normal and diseased tissue at depths of a millimeter or more.

Acknowledgments

References

1. J. P. Meyer and D. Gillat, "What's new in bladder cancer?" *Trends Urol. Gynaecol. Sexual Health* **8**(6), 25–29 (2003).
2. J. Hugosson, "Early diagnosis: state of the art in clinical routine and screening studies," in *Renal, bladder, prostate and testicular cancer: an update: the proceedings of the VIth Congress and Controversies in Oncological Urology*, K. H. Kirth, G. H. Mickisch, and F. H. Schroder, Eds., Parthenon Publishing Group, New York (2001).
3. R. Alfano, C. H. Liu, W. L. Sha, H. R. Zhu, D. L. Akins, J. Cleary, R. Prudente, and E. Cellmer, "Human breast tissue studied by IR Fourier transform Raman spectroscopy," *Lasers Life Sci.* **4**(1), 23–28 (1991).
4. C. Liu, B. B. Das, W. L. Sha Glassmen, G. C. Tang, K. M. Yoo, H. R. Zhu, D. L. Akins, S. S. Lubicz, J. Cleary, R. Prudente, E. Cellmer, A. Caron, and R. R. Alfano, "Raman, fluorescence and time-resolved light scattering as optical diagnostic techniques to separate diseased and normal biomedical media," *J. Photochem. Photobiol., B* **16**(2), 187–209 (1992).
5. A. Mahadevan-Jansen and R. Richards-Kortum, "Raman spectroscopy for the detection of cancers and pre-cancers," *J. Biomed. Opt.* **1**, 31–70 (1996).
6. M. S. Feld, R. Manoharan, J. Salenius, J. Orenstein-Carndona, T. J. Roemer, J. F. Brennan, R. Dasari, and Y. Wang, "Detection and characterization of human tissue lesions with near infra-red Raman spectroscopy," *Proc. SPIE* **2388**, 99-104 (1995).
7. M. Shim, L. M. Song, N. E. Marcon, and B. C. Wilson, "*In vivo* near-infrared Raman spectroscopy: Demonstration of feasibility during clinical gastrointestinal endoscopy," *Photochem. Photobiol.* **72**, 146–150 (2000).
8. C. Kendall, N. Stone, N. Shepherd, K. Geboes, B. Warren, R. Bennett, and H. Barr, "Raman spectroscopy a potential tool for the objective identification and classification of neoplasia in Barrett's oesophagus," *J. Pathol.* **200**, 602–609 (2003).
9. N. Stone, "Raman spectroscopy of biological tissue for application in optical diagnosis of malignancy," PhD Thesis, Cranfield Univ., United Kingdom (2001).
10. T. C. Bakker Schut, M. J. H. Witjes, H. J. C. M. Sterenborg, O. C. Speelman, J. L. N. Roodenburg, E. T. Marple, H. A. Bruining, and G. J. Puppels, "*In vivo* detection of dysplastic tissue by Raman spectroscopy," *Anal. Chem.* **72**, 6010–6018 (2000).
11. B. Schrader, S. Keller, T. Lochte, S. Fendel, D. S. Moore, A. Simon, and I. Sawatzki, "FT Raman spectroscopy in medical diagnostics," *J. Mol. Struct.* **348**, 293–296 (1995).
12. H. Edwards, A. Williams, and B. Barry, "Potential applications of FT-Raman spectroscopy for dermatological diagnosis," *J. Mol. Struct.* **347**, 379–387 (1995).
13. P. Caspers, G. W. Lucassen, R. Wolthuis, H. A. Bruining, and G. J. Puppels, "*In vitro* and *in vivo* Raman spectroscopy of human skin," *Biospectroscopy* **4**, S31–S39 (1998).
14. S. Kaminaka, H. Yamazaki, T. Ito, E. Kohda, and H. Hamaguchi, "Near infrared Raman spectroscopy of human lung tissues: Possibility of molecular-level cancer diagnosis," *J. Raman Spectrosc.* **32**, 139–141 (2001).
15. N. Stone, P. Stravroulaki, C. Kendall, M. Birchall, and H. Barr, "Raman spectroscopy for early detection of laryngeal malignancy—preliminary results," *Laryngoscope* **110**, 1756–1763 (2000).
16. P. Crow, N. Stone, C. A. Kendall, J. S. Uff, J. A. Farmer, H. Barr, and M. P. Wright, "The use of Raman spectroscopy to identify and grade prostatic adenocarcinoma *in vitro*," *Br. J. Cancer* **89**(1), 106–108 (2003).
17. N. Stone, C. Kendall, N. Shepherd, P. Crow, and H. Barr, "Near-infrared Raman spectroscopy for the classification of epithelial precancers and cancers," *J. Raman Spectrosc.* **33**, 564–573 (2002).
18. P. J. Caspers, G. W. Lucassen, E. A. Carter, H. A. Bruining, and G. J. Puppels, "*In vivo* confocal Raman microspectroscopy of the skin: Noninvasive determination of molecular concentration profiles," *J. Invest. Dermatol.* **116**(3), 434–442 (2001).
19. P. Matousek, N. Everall, M. Towrie, and A. W. Parker, "Depth profiling in diffusely scattering media using Raman spectroscopy and picosecond gating," *Appl. Spectrosc.* **59**(2), 200–205 (2005).
20. M. D. Morris, A. E. Goodship, E. R. C. Draper, P. Matousek, M. Towrie, and A. W. Parker, "Kerr-gated picosecond Raman spectroscopy and Raman photon migration of equine bone tissue with 400-nm excitation," *Proc. SPIE* **5321**, 164–169 (2004).
21. P. Matousek, M. Towrie, A. Stanley, and A. W. Parker, "Efficient rejection of fluorescence from Raman spectra using picosecond Kerr gating," *Appl. Spectrosc.* **53**(12), 1485–1489 (1999).
22. P. Matousek, M. Towrie, C. Ma, W. M. Kwok, D. Phillips, A. W. Toner, and A. W. Parker, "Fluorescence suppression in resonance Raman spectroscopy using a high-performance picosecond Kerr gate," *J. Raman Spectrosc.* **32**, 983–988 (2001).
23. D. J. Smithies and P. H. Butler, "Modelling the distribution of laser light in port-wine stains with the Monte Carlo method," *Phys. Med. Biol.* **40**, 701–731 (1995).